Inverted Polymer Solar Cells Integrated with a Low-Temperature-Annealed Sol-Gel-Derived ZnO Film as an Electron Transport Layer

*Yanming Sun, Jung Hwa Seo, Christopher J. Takacs, Jason Seifter, and Alan J. Heeger**

Bulk heterojunction (BHJ) polymer solar cells (PSCs) based on composites of conjugated polymers (electron donor) and fullerene derivatives (electron acceptor) have attracted attention due to their potential as renewable energy sources.[1–7] The major challenges for BHJ solar cells are the achievement of competitive power conversion efficiencies (PCEs) and the demonstration of long-term air stability.[8–16]

BHJ solar cells are typically fabricated with a transparent conductive anode (e.g. indium tin oxide, ITO), a low-work-function metal cathode (e.g., Al, Ca), and an active layer (a mixture of conjugated polymer and fullerene derivative) sandwiched between the anode and cathode. The BHJ layer and cathode dramatically affect the stability. In particular, the cathode is susceptible to degradation by oxygen and water vapor. Poly(3,4-ethylenedioxythiophene):poly(styrene sulfonate) (PEDOT:PSS) is often used as an anode buffer layer. Long-term stability is a problem because PEDOT:PSS is hygroscopic and acidic.[17–21]

In order to circumvent these problems, inverted polymer solar cells have been developed; air-stable high-work-function metals (e.g., Au, Ag) are used as the anode to collect holes and ITO is used as the cathode to collect electrons. In the inverted architecture, n-type metal oxides such as titanium oxide (TiO_x), zinc oxide (ZnO), and cesium carbonate (Cs_2CO_3) are deposited onto the ITO electrode to break the symmetry.[22–24] The elimination of the PEDOT:PSS layer improves the device stability. Moreover, in the inverted cell, the anode is a high-work-function metal such as Ag, which can be formed using coating or printing technology to simplify and lower the cost of manufacturing.[25]

Among the n-type metal oxides used in inverted cells, ZnO is a promising candidate due to its relatively high electron mobility, environmental stability, and high transparency. A variety of fabrication methods have been employed to grow thin films of ZnO. Sol-gel method has been extensively investigated as a solution-based thin-film deposition process.[26] Sol-gel-derived ZnO film is widely used in inverted solar cells. However, a high annealing temperature, usually over 200 °C and incompatible with flexible substrates, is used to promote crystallization and removal of residual organic compounds.[27–29] Although solution-processed ZnO nanoparticles have been shown to be easily processed into thin films via spin coating or roll-to-roll printing at room temperature,[23,30,31] ZnO nanoparticles are not very stable in solution and a ligand is usually used to stabilize them.[32] We report here that uniform sol-gel-derived ZnO films can be obtained at relatively low annealing temperatures (≤200 °C) and they can function as the efficient electron transporting layer in inverted solar cells.

Despite a dramatic improvement of stability, inverted solar cells suffer from relatively lower PCEs compared to conventional solar cells, mainly due to the lack of efficient and air-stable photoactive materials. Recently, BHJ solar cells based on poly[N-9”-hepta-decanyl-2,7-carbazole-alt-5,5-(4’,7’-di-2-thienyl-2’,1’,3’-benzothiadiazole)] (PCDTBT) and [6,6]-phenyl C_{70}-butyric acid methyl ester ($PC_{70}BM$) composites show a PCE in excess of 6%.[9] Moreover, PCDTBT has been demonstrated to be a stable semiconducting polymer.[33] Here, the potential utilization of PCDTBT into inverted solar cells is explored. By integrating with a sol-gel-derived ZnO film as an electron transport layer, inverted PCDTBT:$PC_{70}BM$ solar cells show high efficiency and promising long-term stability. A record high PCE up to 6.33% is demonstrated, and the PCE remains above 70% of the original value even after storage in air for 30 days.

The molecular structures of PCDTBT and $PC_{70}BM$, the inverted cell device structure and the energy levels of the component materials are shown in **Figure 1**. Sol-gel-derived ZnO films were prepared using zinc acetate in 2-methoxyethanol as a precursor solution. The details of synthesis are described in the Experimental Section. The precursor solution was cast onto ITO-glass and subsequently treated at different annealing temperatures (130 °C, 150 °C, and 200 °C) for 1 h during which the precursor was converted to dense ZnO film by hydrolysis. The valence band maximum (VBM) of the ZnO was determined by ultraviolet photoelectron spectroscopy (UPS), and the band gap (E_g) was obtained from the UV absorption edge. The VBM and the conduction band minimum (CBM) of the ZnO film are 7.68 ± 0.03 eV and 4.33 ± 0.07 eV, respectively. As shown in Figure 1c, because the CBM is close to the energy of the lowest unoccupied molecular orbital (LUMO) of $PC_{70}BM$, electron transport to the ITO cathode is expected. A stable molybdenum oxide (MoO_x) thin film was selected as the hole extraction layer. The VBM of MoO_x is 5.6 eV (determined by UPS), which is close to the highest occupied molecular orbital (HOMO) of PCDTBT. Thus, holes can be efficiently transported to the Ag anode without significant loss in energy.

In order to characterize the composition of sol-gel-derived ZnO films, the X-ray photoelectron spectroscopy (XPS) measurements were carried out. **Figure 2** shows core level XPS spectra of Zn 2p and O 1s for the sol-gel-derived ZnO films

Dr. Y. M. Sun, Dr. J. H. Seo, C. J. Takacs, J. Seifter, Prof. A. J. Heeger
Center for Polymers and Organic Solids
University of California
Santa Barbara, California 93106, USA
E-mail: ajhe@physics.ucsb.edu

DOI: 10.1002/adma.201004301

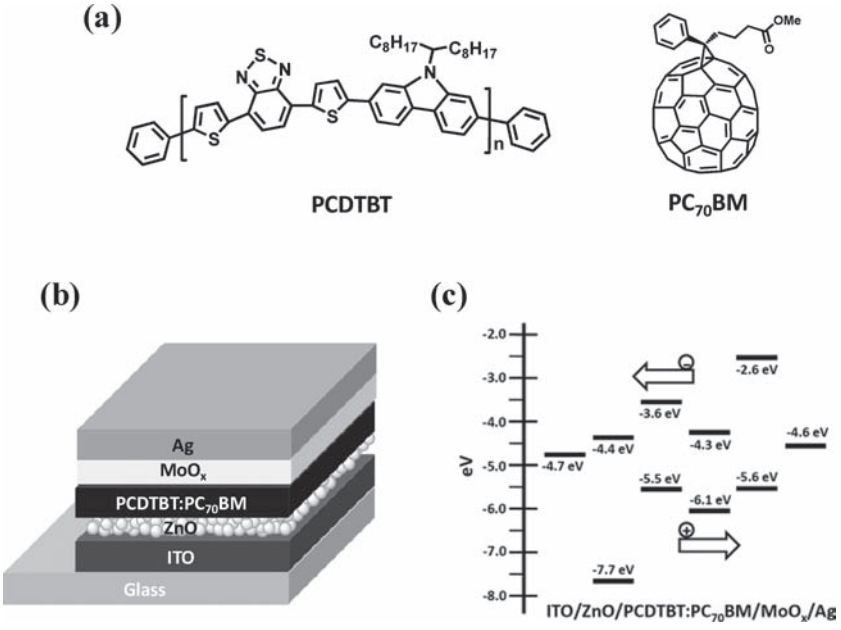

Figure 1. a) The molecular structures of PCDTBT and $PC_{70}BM$. b) The device structure of the inverted PCDTBT:$PC_{70}BM$ solar cell. c) Energy level diagram of the component materials used in device fabrication.

annealed at various temperatures. From Figure 2a, the binding energy of Zn $2p_{3/2}$ peak was at 1022.7 eV in the ZnO films annealed at 130 °C.[34–36] Complete Zn 2p XPS spectra are shown in the Supporting Information. The maximum of the Zn $2p_{3/2}$ peak shifts toward lower binding energy by 0.2 eV as the annealing temperature is increased up to 200 °C; the shift implies that more Zn atoms are bound to O atoms.[34]

The O 1s XPS spectra exhibit asymmetric line shapes (Figure 2b). The peak with lower binding energy (531.4 eV) corresponds to O atoms in a ZnO matrix. The second peak, at 533.0 eV, is attributed to an oxygen-deficient component (for example, zinc hydroxide, $Zn(OH)_2$).[37,38] The main peak shifts towards lower energy by 0.2 eV after annealing at 200 °C. From the decreased intensity of the higher binding energy component, we infer that the oxygen-deficient component decreases with annealing. The relative magnitude of the low-binding-energy O atoms was 53% when annealed at 130 °C and increased to 60% after annealing at 200 °C. Therefore, annealing decreases the oxygen-deficient component and increases the number of Zn–O bonds in the sol-gel-derived ZnO film, leading to deviation from 1:1 stoichiometry. From the XPS survey spectra, the atomic concentrations of Zn and O were obtained; 1:1.12 for a 130 °C anneal and 1:1.22 for a 200 °C anneal.

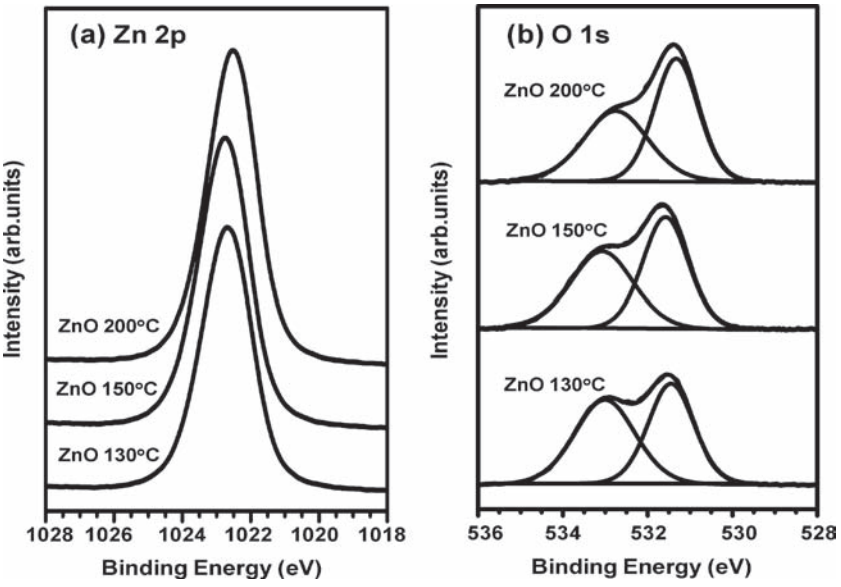

Figure 2. a) Zn 2p and b) O 1s XPS spectra of of ZnO films with different annealing temperatures.

The surface roughness of the ZnO film and the topography of PCDTBT:$PC_{70}BM$ composite were investigated by atomic force microscopy (AFM). As shown in **Figure 3**, uniform ZnO films composed of small grains are observed. The root mean square (RMS) roughness values are 1.24 nm, 0.80 nm, and 1.29 nm for ZnO films annealed at 130 °C, 150 °C, 200 °C, respectively. However, PCDTBT:$PC_{70}BM$ films deposited onto the ZnO/ITO glass substrates are insensitive to the ZnO surface topography; the average RMS roughness is 0.54 nm.

Current density–voltage (J–V) characteristics of inverted solar cells incorporating ZnO films with different annealing temperatures under AM 1.5 G irradiation with irradiation intensity of 100 mW cm^{-2} and in dark are shown in **Figure 4**. **Table 1** summarizes the data. There is no significant difference in device performance when ZnO films were annealed at 150 °C and 200 °C (PCE ≈ 6%). However, devices with ZnO film annealed at 130 °C show a reduced PCE (5.4%) with lower short-circuit current density (J_{sc}), open circuit voltage (V_{oc}), and a higher series resistance (R_s). Incident photon-to-current efficiency (IPCE) spectra are shown in Figure 4b. For devices comprising ZnO film annealed at either 150 °C or 200 °C, the maxmium IPCE is 68%, which is indicative of efficient photon-to-electon conversion. Please note that the integrated IPCE values are always in good agreement with the measured short-circuit current within a few percent.

To get additional insight into the device performance, we examined the charge transport properties of the sol-gel-derived ZnO films. Electron mobilities were obtained from field-effect transistors (FETs) fabricated with ZnO as the semiconducting layer in the channel (details are provided in the Supporting Information). Although X-ray diffraction (XRD) measurements show no crystallinity (2θ in the range of 30 to 70 degrees), the electron mobility increases with increasing annealing temperatures (see Table 1).

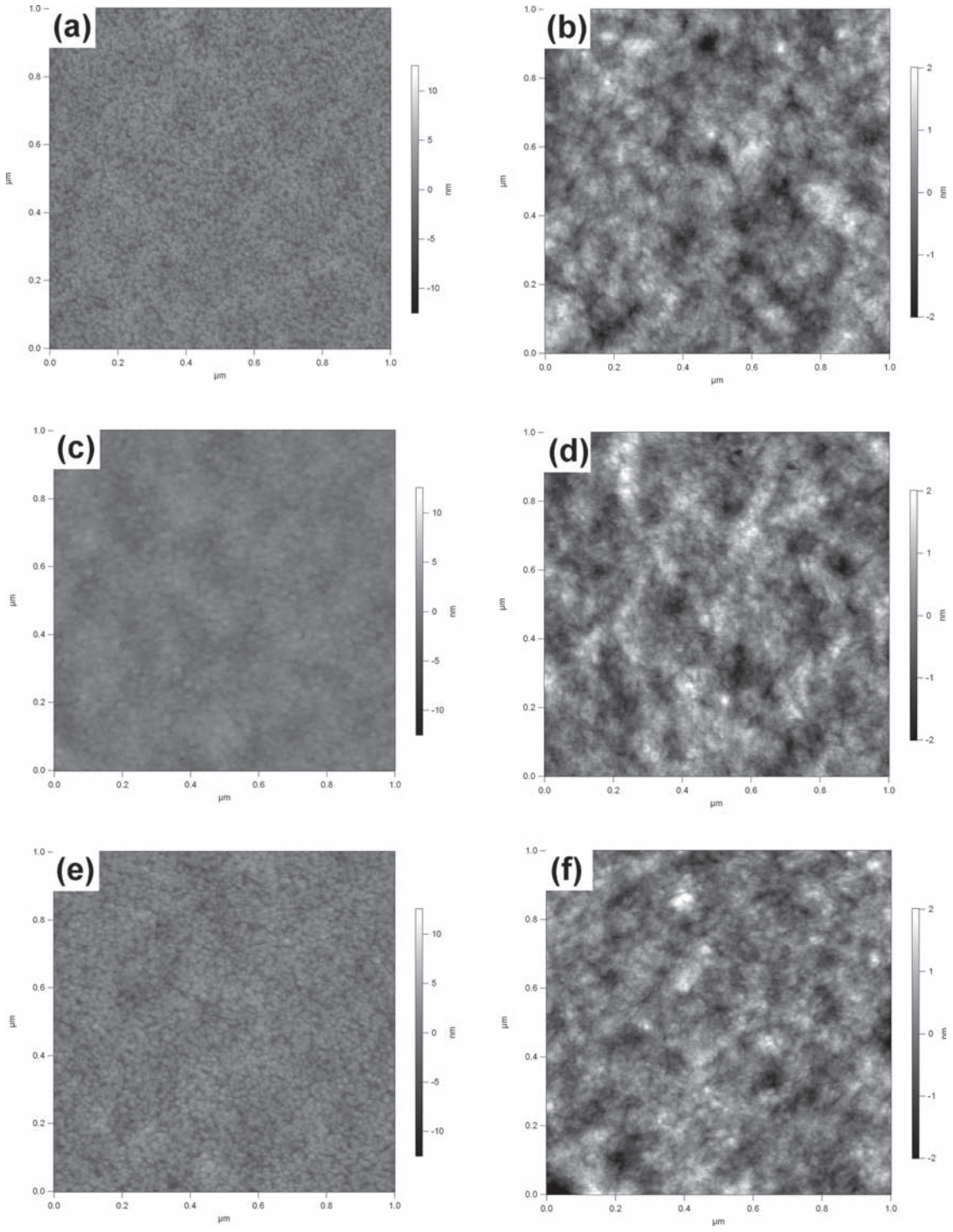

Figure 3. AFM images of ZnO fims with the following annealing temperaures: a) 130 °C, c) 150 °C, and e) 200 °C. Topography images of PCDTBT:$PC_{70}BM$ active layer on top of ZnO films with the following annealing temperaures: b)130 °C, d) 150 °C, and f) 200 °C.

The use of metal oxides on both sides of the PCDTBT:$PC_{70}BM$ layer prevents the diffusion of moisture into the active layer. The stability of the inverted PCDTBT:$PC_{70}BM$ solar cells (with MoO_x as the hole transport layer and ZnO as the electron transport layer) is shown in Figure 4d. The solar cells were exposed continuously to air at room temperature (without any encapsulation barrier). The PCEs remain above 70% of the original value even after storage in air for more than 30 days. Note that because the HOMO of PCDTBT is 5.5 eV below the vacuum, PCDTBT is

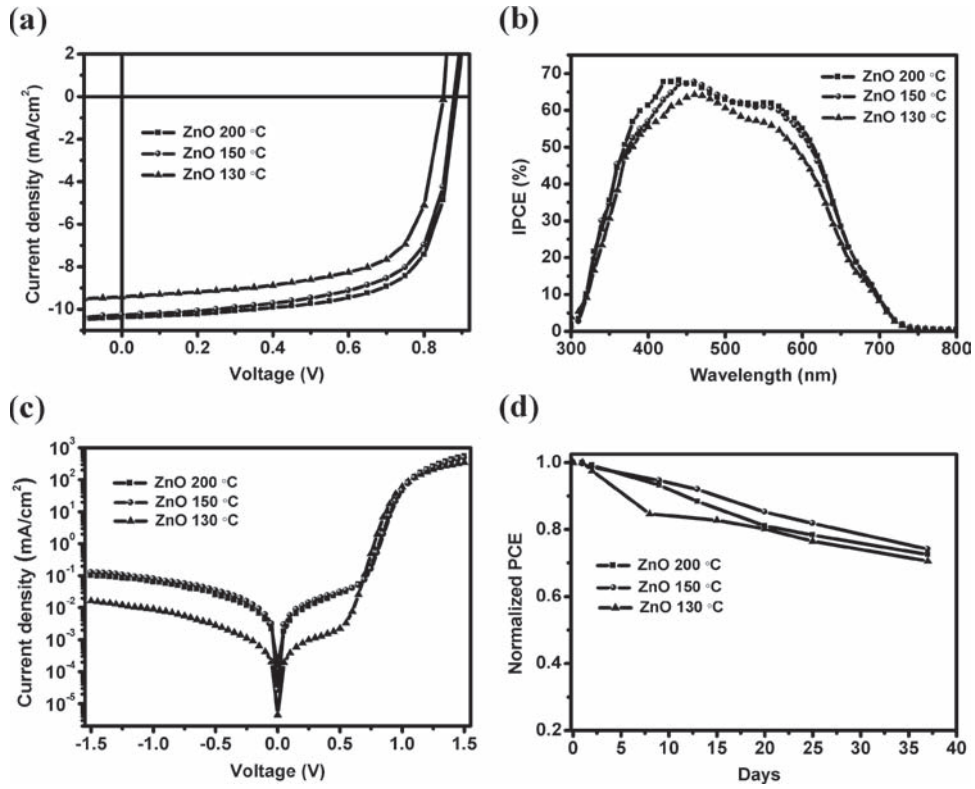

Figure 4. a) *J–V* characteristics of inverted PCDTBT:$PC_{70}BM$ solar cells incorporating ZnO films with the indicated annealing temperatures. b) IPCE spectra of inverted PCDTBT:$PC_{70}BM$ solar cells. c) Dark current of inverted PCDTBT:$PC_{70}BM$ solar cells. d) Normalized PCEs for inverted PCDTBT:$PC_{70}BM$ solar cells as a function of storage time in air under ambient conditions.

Table 1. Characteristics of sol-gel-derived ZnO films with different annealing temperatures and the device performance parameters of inverted PCDTBT:$PC_{70}BM$ solar cells fabricated with ZnO film as the electron transport layer.

Device	VBM [eV]	CBM [eV]	μ [$cm^2\ V^{-1}\ s^{-1}$]	V_{oc} [V]	J_{SC} [mA cm^{-2}]	*FF* [%]	PCE [%]		R_s [Ω cm^2]
							Best	Average[a)]	
ZnO 130 °C	–7.65	–4.27	2.0×10^{-4}	0.85	9.42	66.9	5.36	5.10	1.88
ZnO 150 °C	–7.65	–4.31	2.8×10^{-3}	0.88	10.27	66.8	6.03	5.86	1.00
ZnO 200 °C	–7.71	–4.40	4.0×10^{-3}	0.88	10.41	68.8	6.33	6.08	0.84

[a)]The parameters of PCEs were averaged over ten solar cells.

relatively stable against oxidation in ambient conditions.[33] Nevertheless, for PCDTBT:PCBM cells in the traditional architecture, the PCE decreases significantly when exposed to air and the PCE is reduced by a factor of 2 after air exposure for 16 h.

In conclusion, efficient, air-stable inverted BHJ solar cells fabricated with a low-temperature annealed sol-gel-derived ZnO film as an electron transport layer have been demonstrated. Power conversion efficiencies of approximately 6% are demonstrated. The solar cells are stable due to the combination of the air-stable semiconducting polymer (PCDTBT) and the metal oxide transport layers (ZnO as the electron transport layer and MoO_x as the hole transport layer). The low annealing temperature (≤200 °C) used to grow the ZnO film is compatible with fabrication on flexible substrates. The results define a promising pathway for the fabrication of polymer solar cells with high efficiency and long-term stability

Experimental Section

Preparation of the ZnO Precursor: The ZnO precursor was prepared by dissolving zinc acetate dihydrate ($Zn(CH_3COO)_2{\cdot}2H_2O$, Aldrich, 99.9%, 1 g) and ethanolamine ($NH_2CH_2CH_2OH$, Aldrich, 99.5%, 0.28 g) in 2-methoxyethanol ($CH_3OCH_2CH_2OH$, Aldrich, 99.8%, 10 mL) under vigorous stirring for 12 h for the hydrolysis reaction in air.

Fabrication of Inverted PSCs: Inverted solar cells were fabricated on ITO-coated glass substrates. The ITO-coated glass substrates were first cleaned with detergent, ultrasonicated in water, actone and isopropyl alcohol, and subsequently dried overnight in an oven. The ZnO precursor solution was spin-cast on top of the ITO-glass substrate. The films were annealed at 130 °C, 150 °C, or 200 °C for 1 h in air. The ZnO film

thickness was approximately 30 nm, as determined by a profilometer. The ZnO-coated substrates were transferred into a glove box. A solution containing a mixture of PCDTBT:$PC_{70}BM$ (1:4) in a mixed solvent (dichlorobenzene:chlorobenzene = 3:1) with a concentration of 7 mg mL^{-1} was spin-cast on top of ZnO films with thickness of approximately 70 nm. The polymer–fullerene films were heated at 70 °C for 10 min. Then, a thin layer of MoO_x film (≈6 nm) was evaporated on top of the active layer. Finally, the anode (Ag, ≈60 nm) was deposited through a shadow mask by thermal evaporation in a vacuum of about 3×10^{-6} Torr. The active area of device was 4.5 mm^2. *J–V* characteristics were measured using a Keithley 236 source measure unit. Solar cell performance was measured using an Air Mass 1.5 Global (AM 1.5 G) solar simulator with an irradiation intensity of 100 mW cm^{-2}. The spectral mismatch factor was calculated by comparison of the solar simulator spectrum and the AM 1.5 spectrum at room temperature. The IPCE spectra for the inverted structure PSCs were measured on an IPCE measuring system.

Fabrication of FET Devices: All FET devices were fabricated on heavily n-type doped silicon (Si) wafers with a 200-nm-thick thermally grown SiO_2 layer. The ZnO precursor solution was spin-cast on top of the untreated SiO_2 surface. Then, the films are annealed at 130 °C, 150 °C, or 200 °C for 1 h in air. The samples were then transferred into a glove box, and Al source and drain electrodes (≈60 nm) were deposited by thermal evaporation using a shadow mask. The channel length (*L*) and channel width (*W*) were 50 μm and 1.5 mm, respectively. Electrical characterization was done using a Keithley semiconductor parametric analyzer (Keithley 4200). All measurements were performed in a glove box.

Thin Film Characterization: The UV-vis absorption and transmission measurements of ZnO films deposited onto quartz substrates were recorded at room temperature with an Agilent 8453 spectrophotometer. AFM imaging was carried out in air using an Asylum Research MFP-3D AFM. XRD measurements were carried out in air on a Philips Xpert MPD Diffractometer with a Cu Kα source (wavelength of 1.5405 Å). The XPS and UPS measurements were performed in a Kratos Ultra Spectrometer (a base pressure of 1×10^{-9} Torr) using monochromatized Al Kα X-ray photons ($h\nu$ = 1486.6 eV for XPS) and He I (21.2 eV for UPS) discharge lamp. ZnO films were deposited on top of ITO substrates by spin-casting in air. The pass energy and a step size were 40 eV and 0.05 eV for XPS and 10 eV and 0.025 eV for UPS. For XPS data, curve fitting and linear background subtraction were done using CASA XPS (version 2.3) software. For UPS, a sample bias of –9 V was used in order to separate the sample and the secondary edge for the analyzer. All samples were kept inside a high vacuum chamber overnight to remove solvent.

Supporting Information

Supporting Information is available from the Wiley Online Library or from the author.

Acknowledgements

The authors are grateful to Dr. Wei Lin Leong for important discussions. This research was supported by the US Army General Technical Services (LLC/GTS-S-09-1-196) and by the Air Force Office of Scientific Research (AFOSR FA9550-08-1-024, Charles Lee Program Officer). The authors thank Dr. David Waller (Konarka Technologies, Inc) for providing the PCDTBT material.

Received: November 21, 2010
Published online: Febuary 22, 2011

[1] N. S. Sariciftci, L. Smilowitz, A. J. Heeger, F. Wudl, *Science* **1992**, *258*, 1474.
[2] G. Yu, J. Gao, J. C. Hummelen, F. Wudl, A. J. Heeger, *Science* **1995**, *270*, 1789.
[3] P. W. M. Blom, V. D. Mihailetchi, L. J. A. Koster, D. E. Markov, *Adv. Mater.* **2007**, *19*, 1551.
[4] S. Günes, H. Neugebauer, N. S. Sariciftci, *Chem. Rev.* **2007**, *107*, 1324.
[5] G. Dennler, M. C. Scharber, C. J. Brabec, *Adv. Mater.* **2009**, *21*, 1323.
[6] L. M. Chen, Z. Hong, G. Li, Y. Yang, *Adv. Mater.* **2009**, *21*, 1434.
[7] F. C. Krebs, T. D. Nielsen, J. Fyenbo, M. Wadstrøm, M. S. Pedersen, *Energy Environ. Sci.* **2010**, *3*, 512.
[8] Y. Liang, L. Yu, *Acc. Chem. Res.* **2010**, *43*, 1227.
[9] S. H. Park, A. Roy, S. Beaupré, S. Cho, N. Coates, J. S. Moon, D. Moses, M. Leclerc, K. Lee, A. J. Heeger, *Nat. Photonics* **2009**, *3*, 297.
[10] N. Blouin, A. Michaud, D. Gendron, S. Wakim, E. Blair, R. Neagu-Plesu, M. Belletête, G. Durocher, Y. Tao, M. Leclerc, *J. Am. Chem. Soc.* **2008**, *130*, 732.
[11] W. L. Ma, C. Y. Yang, X. Gong, K. Lee, A. J. Heeger, *Adv. Funct. Mater.* **2005**, *15*, 1617.
[12] G. Li, V. Shrotriya, J. Huang, Y. Yao, T. Moriarty, K. Emery, Y. Yang, *Nat. Mater.* **2005**, *4*, 864.
[13] J. Peet, J. Y. Kim, N. E. Coates, W. L. Ma, D. Moses, A. J. Heeger, G. C. Bazan, *Nat. Mater.* **2007**, *6*, 497.
[14] J. A. Hauch, P. Schilinsky, S. A. Choulis, R. Childers, M. Biele, C. J. Brabec, *Sol. Energy Mater. Sol. Cells* **2008**, *92*, 727.
[15] C. Lungenschmied, G. Dennler, H. Neugebauer, S. N. Sariciftci, M. Glatthaar, T. Meyer, A. Meyer, *Sol. Energy Mater. Sol. Cells* **2007**, *91*, 379.
[16] C. J. Brabec, S. Gowrisanker, J. J. M. Halls, D. Laird, S. Jia, S. P. Williams, *Adv. Mater.* **2010**, *22*, 3839.
[17] K. Kawano, R. Pacios, D. Poplavskyy, J. Nelson, D. D. C. Bradley, J. R. Durrant, *Sol. Energy Mater. Sol. Cells* **2006**, *90*, 3520.
[18] M. P. de Jong, L. J. van IJzendoorn, M. J. A. de Voigt, *Appl. Phys. Lett.* **2000**, *77*, 2255.
[19] M. Jørgensen, K. Norrman, F. C. Krebs, *Sol. Energy Mater. Sol. Cells* **2008**, *92*, 686.
[20] H. Yan, P. Lee, A. G. Armstrong, G. A. Evmenenko, P. Dutta, T. J. Marks, *J. Am. Chem. Soc.* **2005**, *127*, 3172.
[21] K. Norrman, S. A. Gevorgyan, F. C. Krebs, *ACS Appl. Mater. Interfaces* **2009**, *1*, 102.
[22] C. Waldauf, M. Morana, P. Denk, P. Schilinsky, K. Coakley, S. A. Choulis, C. J. Brabec, *Appl. Phys. Lett.* **2006**, *89*, 233517.
[23] M. S. White, D. C. Olson, S. E. Shaheen, N. Kopidakis, D. S. Ginley, *Appl. Phys. Lett.* **2006**, *89*, 143517.
[24] G. Li, C.-W. Chu, V. Shrotriya, J. Huang, Y. Yang, *Appl. Phys. Lett.* **2006**, *88*, 253503.
[25] F. C. Krebs, *Sol. Energy Mater. Sol. Cells* **2009**, *93*, 465.
[26] M. N. Kamalasanan, S. Chandra, *Thin Solid Films* **1996**, *288*, 112.
[27] A. K. K. Kyaw, X. W. Sun, C. Y. Jiang, G. Q. Lo, D. W. Zhao, D. L. Kwong, *Appl. Phys. Lett.* **2008**, *93*, 221107.
[28] C.-H. Hsieh, Y.-J. Cheng, P.-J. Li, C.-H. Chen, M. Dubosc, R.-M. Liang, C.-S. Hsu, *J. Am. Chem. Soc.* **2010**, *132*, 4887.
[29] S. K. Hau, H.-L. Yip, N. S. Baek, J. Zou, K. O'Mellay, A. K.-Y. Jen, *Appl. Phys. Lett.* **2008**, *92*, 253301.
[30] F. C. Krebs, S. A. Gevorgyan, J. Alstrup, *J. Mater. Chem.* **2009**, *19*, 5442.
[31] J. Gilot, I. Barbu, M. M. Wienk, R. A. Janssen, *Appl. Phys. Lett.* **2007**, *91*, 113520.
[32] F. C. Krebs, Y. Thomann, R. Thomann, J. W. Andreasen, *Nanotechnology* **2008**, *19*, 424013.
[33] S. Cho, J. H. Seo, S. H. Park, S. Beaupré, M. Leclerc, A. J. Heeger, *Adv. Mater.* **2010**, *22*, 1253.
[34] M. Chen, X. Wang, Y. H. Yu, Z. L. Pei, X. D. Bai, C. Sun, R. F. Huang, L. S. Wen, *Appl. Surf. Sci.* **2000**, *158*, 134.
[35] H. Sakata, Y. Natsume, *Thin Solid Films* **2000**, *372*, 30.
[36] Q. Wan, K. Yu, T. H. Wang, C. L. Lin, *Appl. Phys. Lett.* **2003**, *83*, 2253.
[37] Y. Zhang, G. Du, X. Wang, W. Li, X. Yang, Y. Ma, B. Zhao, H. Yang, D. Liu, S. Yang, *J. Crystal Growth* **2003**, *252*, 180.
[38] X. Q. Wei, B. Y. Man, M. Liu, C. S. Xue, H. Z. Zhuang, C. Yang, *Physica B* **2007**, *388*, 145.